Conformational stability of cyclopropanecarboxaldehyde is ruled by vibrational effects

Conformational stability of cyclopropanecarboxaldehyde is ruled by vibrational effects

Silvia Alessandrini[a,b], Mattia Melosso[b], Ningjing Jiang[b], Luca Bizzocchi[a,b], Luca Dore[b], and Cristina Puzzarini[b]

[a]Scuola Normale Superiore, Piazza dei Cavalieri 7, I-56126 Pisa, Italy; [b]Dipartimento di Chimica "Giacomo Ciamician", Università di Bologna, Via F. Selmi 2, I-40126 Bologna, Italy.

ARTICLE HISTORY
Compiled June 15, 2023

ABSTRACT

Cyclopropanecarboxaldehyde (CPCA) has two main conformers, *syn* and *anti*, that are renowned for being very close in energy. The relative stability of these two main species is constantly reversed by changing the level of theory or the experimental technique employed in its determination. The *anti* conformer is predicted to be the most favoured in condensed states of matter, but uncertainty still remains on the relative stability in the gas phase. To gain further insights into this issue, the investigation of the rotational spectrum of both *syn*- and *anti*-CPCA has been extended in the 246-294 GHz frequency region and complemented by a detailed computational study of both conformers. A fit incorporating the recorded rotational transitions as well as those reported in the literature led to the accurate determination of the rotational parameters, also including high-order centrifugal distortion constants. Accurately computed vibrational frequencies were used to re-analyse the infrared spectrum of both conformers, thereby allowing a re-assignment of two vibrational bands, namely ν_4 of *anti*-CPCA and ν_{26} of the *syn* conformer. While our state-of-the-art computations favour the *anti* conformer in the stability order, estimates from analysis of rotational spectra are rather controversial and are strongly affected by several factors, such as the zero-point vibrational correction.

KEYWORDS
rotational spectroscopy; vibrational analysis; conformer stability; cyclopropanecarboxaldehyde; computational spectroscopy

1. Introduction

Within the large chemical space associated to stereochemistry, the interconversion occurring along the rotation of a sigma bond is quite common and gives rise to various conformations of the species under consideration [1]. In the domain of the Born-Oppenheimer (BO) approximation [2], the conformations that are minima on the potential energy surface (PES) are denoted as conformers (also known as conformational isomers) and interconvert between each other via transition states (TSs), which are conformations of the specific molecule as well. Thus, conformers can be obtained without cleavage of bonds, unlike configurational and geometric isomers, which are different stereochemical features [1]. The immediate consequence is that several

Corresponding author S. A. Email: silvia.alessandrini@sns.it

conformers coexist in a sample, and they are in dynamical equilibrium, with the relative abundances being ruled by three main physicochemical characteristics. These are the energetic rotational barrier required for the interconversion and, somewhat correlated to the former point, the temperature of the sample, i.e. the energy available to the system. Indeed, above a certain temperature, the system has more energy than that required for overcoming the interconversion barrier, thus leading to the so-called free-rotation condition [1]. The last but not the least characteristic to consider is the state of the sample, e.g. solid, liquid or gas, which can favour one conformer with respect to the others. For example, intermolecular interactions that are present in the solid state can preferentially stabilise one conformer with respect to another [3, 4].

Experiments offer the opportunity to look into the relative conformers population in a sample via measurable quantities. In the field of spectroscopy, with particular reference to rotational and/or vibrational spectroscopic techniques, the intensity of transition lines can be used to identify the most stable species. Rotational spectroscopy can only be carried in the gas phase, while infrared and Raman spectroscopies can handle both condensed and gaseous sample. However, the high resolution required for obtaining good estimates of line intensities is achievable only in gas-phase experiments [5, 6]. As in the case of line positions, experimental determinations often need to be supported and/or complemented by quantum-chemical calculations. In the present case, the analysis of the PES allows the identification of all possible conformers and of the TSs ruling their interconversion, and thus permits the estimate of the corresponding rotational barriers [6–9]. Overall, quantum-chemical computations allow the theoretical derivation of the relative abundances of each conformer at a given temperature. The interplay of experiment and theory is crucial whenever experiments alone are unable to reveal the observed conformer, as shown — for example — in refs. [6, 10–12].

The present work, a joint rotational spectroscopy–quantum chemistry study, aims at providing new insights into cyclopropanecarboxaldehyde's (CPCA) *syn* and *anti* conformers. As well-known from the literature [13–15], they lie very close in terms of electronic energy. These conformers are obtained through the rotation of the bond between the aldehydic carbon and the adjacent C_α and differ for the OCCH dihedral angle as schematically depicted in Fig. 1. Both species belong to the C_s point group.

The first study on CPCA dates back to 1971, when Volltrauer and Schwendeman [16] reported its microwave spectrum in the 8-32 GHz frequency range. From the intensity of the rotational transitions, the authors [16] estimated a *syn*-*anti* relative energy of 0.12 kJ mol^{-1} in the gas phase, with an error bar of 0.24 kJ mol^{-1}. The authors also evaluated the barrier for interconversion to be 18.4 ± 4.8 kJ mol^{-1}. Further determinations were reported about 20 years later by Durig et. al. [13, 17], who assigned the vibrational spectra of *syn* and *anti*-CPCA. In their work, the *syn* species is reported as the most stable conformer in the gas phase, with the *anti* conformer lying 0.72 kJ mol^{-1} higher in energy. However, in the liquid phase, the stability appears to be reversed and the *anti* species is the most stable [13]. This only apparent difference is justified by the stronger dipole moment of the *anti* conformer with respect to *syn*, which allows the formation of stronger intermolecular interactions in the condensed phase [3, 4, 13]. The stability of CPCA conformers was also analysed by NMR spectroscopy in a freon matrix at T=103 K and the results clearly point out a larger stability of the *anti* conformer with respect to *syn*, with an energy barrier of 21.0 kJ mol^{-1} [18]. The isomerisation kinetics of CPCA was directly investigated in a dynamical rotational spectroscopy (DRS) experiment [14, 19] via broadband microwave spectroscopy. As reported in ref. [14], this new technique allowed the observation of the isomerisation occurring in a 180 ps scale, with experimental rate constants of 3.08 ×

10^9 s^{-1} for the *anti* to *syn* isomerisation and 2.52×10^9 s^{-1} for the reversed reaction. These estimates are in great contrast with the theoretical ones that predict a 16 times faster process [14, 20]. In the literature, this discrepancy is generally attributed to the presence of "nonstatistical effects" governing the interconversion [14, 20]. The reader is referred to refs. [14, 20] for a detailed account.

Concerning the computational analysis of CPCA, several studies have been reported in literature [15, 20, 21]. The *syn* species is generally predicted to be the most stable species at the equilibrium (i.e. when considering the electronic energy at the bottom of the PES well), the two isomers being however very close in energy and reversing their stability once the zero-point energy (ZPE) is accounted for. To give an example, at the highest level of theory reported in the literature, namely a focal point analysis including extrapolated coupled-cluster energies with fully augmented basis sets and ZPE corrections, the *anti* conformer is favoured by 0.02 kJ mol^{-1} with respect to the *syn* form [20]. Furthermore, as evident from refs. [20] and [15], density functional theory always favours the *anti* conformer. The recent paper of Cabezas et al. [15] was published when our work was already at an advanced stage. There, an extension of the CPCA rotational spectrum up to 116.5 GHz was reported and accompanied by its astronomical search in the high-mass star-forming regions Orion KL and Sgr B2(N). Based on the new experimental measurements, in ref. [15], the *syn*/*anti* stability was re-examined inferring that, in the gas phase, the *anti* isomer lies 0.53 kJ mol^{-1} below the *syn* conformer.

Our work presents a further extension in the investigation of the experimental rotational spectrum, with a global fit including also the recently reported lines [15]. Furthermore, more accurate results on the *syn*/*anti* stability from both the experimental and computational point of view are provided, with a special focus on the vibrational effects.

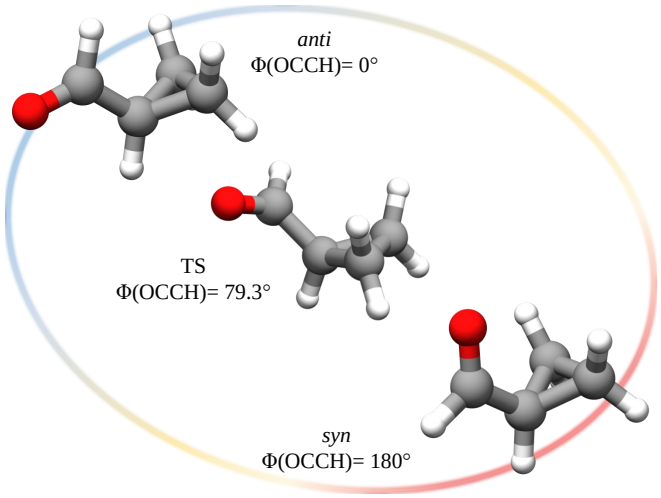

Figure 1. Schematic representation of the *syn* and *anti* conformers of CPCA, together with the TS ruling their interconversion. The Φ(OCCH) indicates the dihedral angle formed by the oxygen atom, the aldehydic carbon, the adjacent C_α and the H atom bonded to it.

2. Experiment

The rotational spectrum of CPCA has been recorded between 246 and 294 GHz with a frequency-modulation millimetre spectrometer, described in details elsewhere [22, 23]. In the current work, the spectrometer was equipped with a Gunn diode (J.E. Carlstrom Co., 80–115 GHz) coupled to a Virginia Diodes wide-band tripler (WR3.4x3, 220–330 GHz) as primary source of radiation. The phase and frequency stability of the radiation is governed by a phase-lock loop, in which the Gunn diode radiation is mixed with a local oscillator and their frequency difference is compared with a 75 MHz reference signal produced by a synthesizer (HP8642A). The latter also provides the frequency modulation of the output radiation at $f = 48$ kHz.

Measurements were performed with a dynamic pressure of about 10 mTorr of CPCA vapors (from the liquid sample) in a free-space absorption glass cell (3 m length); the liquid CPCA was kept in a water/ice bath in order to reduce its vapor pressure. The detection system consists of a Virginia Diodes zero-bias detector (WR3.4ZBD, 220–330 GHz), a +60 dB pre-amplifier, and a lock-in amplifier. The latter was set at twice the modulation frequency ($2f$ detection scheme) and used as a resistor–capacitor circuit with a time constant of 10 ms. All spectra were acquired using a modulation depth of 450 kHz, a frequency step of 42 kHz, and a scan rate of 5 MHz/s for a total integration time of 10.5 h. Under these experimental conditions, the line-center frequency accuracy is expected to be 20–50 kHz.

The recorded spectra present a dozen of consecutive a-type R branch transitions for both CPCA conformers. Owing to the greater μ_a component ($\mu_a \sim 3.2$ D and 2 D for *anti* and *syn*, respectively [16]), the spectral features of *anti*-CPCA are predominant. However, *syn*-CPCA also shows a bright b-type spectrum characterized by strong ${}^rQ$ branches, while the c-type spectrum of the *anti* conformer is too weak to be identified at first sight. Nonetheless, the good signal-to-noise ratio of our spectra enabled the assignment of few tens of μ_c-allowed transitions.

To guide the interpretation of the observed spectrum, ref. [15] being not available at that time, initial spectral predictions were obtained using the rotational constants from Volltrauer and Schwendeman [16] augmented by the quartic and sextic centrifugal distortion parameters computed in this work (see Section 3). The assignment procedure was accomplished using the `PGOPHER` software [24], which allows for simulating rotational spectra and comparing them against the experimental ones in a efficient way. First, the a-type spectra of both conformers have been targeted. The $\Delta J = +1$ transitions form recognizable cluster of lines at high K_a values (see panel **A** of Fig. 2), with the asymmetry splittings generally resolved at $K_a \leq 6$. Thanks to relatively small A rotational constants and moderately high μ_a components, transitions up to $K_a = 43$ and 30 were detectable for *anti*- and *syn*-CPCA, respectively.

For a pinpoint search, the spectral predictions were iteratively updated by adjusting the values of the spectroscopic constants on the basis of the newly-assigned transitions, thus reducing the discrepancy between the simulated and experimental spectra. As a second step, the b-type spectrum of *syn*-CPCA was analysed. In this frequency region, dense clusters of lines spaced by $[A-(B+C)/2] \times (K'_a + K''_a)$ are visible. The spectral pattern observed is similar to the a-type spectrum, but in this case those transitions that have the same K'_a and K''_a, are grouped at low J values and vanish in intensity towards lower frequencies (see panel **B** of Fig. 2).

Finally, the weak c-type transitions of *anti*-CPCA were searched once the uncertainty on its spectroscopic constants was greatly reduced. At this stage, the spectral predictions were sufficiently accurate (few tens of kHz) to secure the identification of

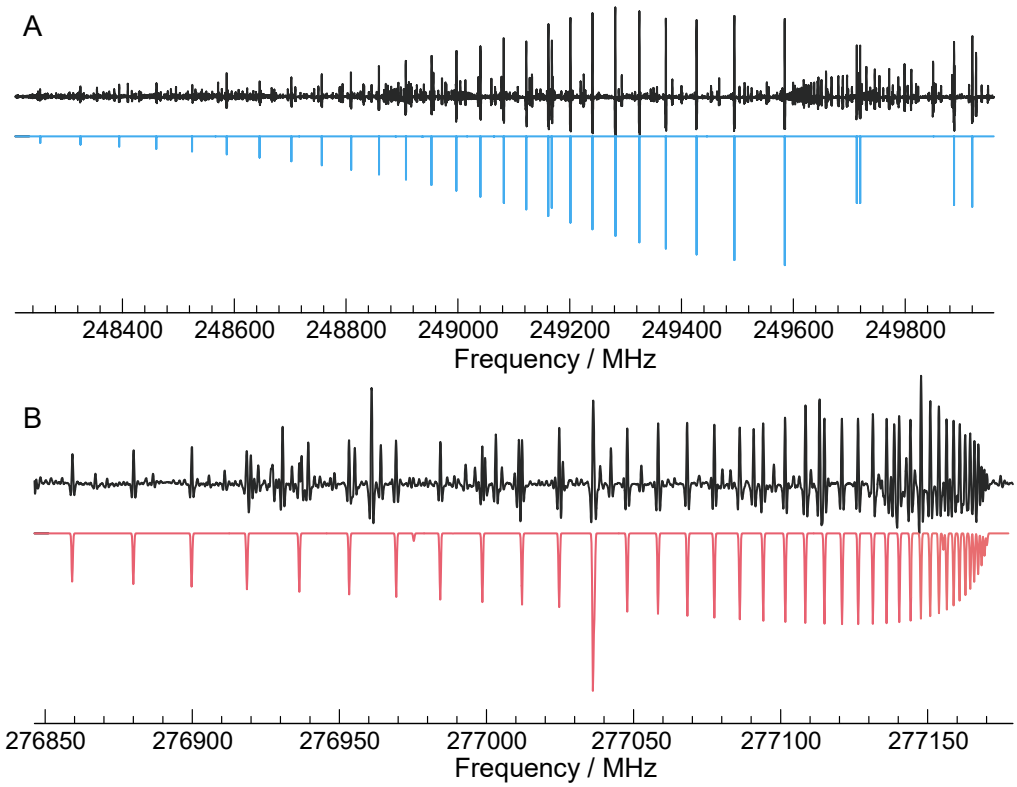

Figure 2. Portion of the experimental rotational spectrum of *anti* (blue lines, panel **A**) and *syn* (red lines, panel **B**) conformers of CPCA. Panel **A** shows the K_a-structure of the *a*-type $J = 40 \leftarrow 39$ transition of *anti*-CPCA, while panel **B** illustrates a *b*-type Q branch of *syn*-CPCA for $K_a = 19 \leftarrow 18$.

such weak features in a spectrum that is quite rich in vibrational satellites [15].

3. Computational Details

The computational characterization of CPCA aimed at refining the energetic considerations on the conformational stability, but also to support experimental measurements in the millimetre-wave region. Indeed, in such frequency range the centrifugal distortion constants strongly affect the peak positions and, prior to the work of Cabezas et al. [15], no estimates of such parameters were reported in the literature. In the view of simulating a rotational spectrum, the first parameters to be derived are the rotational constants, then followed by the centrifugal distortion constants [8, 25, 26]. The former are obtained in a two steps procedure: initially, accurate geometry optimizations are used to straightforwardly retrieve the equilibrium rotational constants of the *syn* and *anti* conformers, then the corresponding vibrational corrections are added. These require the computation of the vibration-rotation interaction constants and, within the second order vibrational perturbation theory (VPT2) formalism, they imply the evaluation up to the third derivatives of the electronic energy with respect to the nuclear displacements, i.e. the cubic force field [25]. Since anharmonic force-field calculations are computationally expensive, they are carried out at a lower level of theory with respect to geometry optimizations. Such a reduction of the computational level does not

significantly affect the accuracy of the overall rotational constants because vibrational corrections amount to 1-3% of the rotational constant value [27].

In the present work, geometry optimizations have been carried out using the composite scheme denoted as"CBS+CV", which is based on coupled cluster (CC) theory [28] with iterative single and double excitations (CCSD) and the perturbative contribution of triples, i.e. the CCSD(T) method [29]. In the "CBS+CV" approach, the energy gradient ($dE_{\mathrm{CBS+CV}}/dx$) to be minimized consists of three contributions [30]:

$$\frac{dE_{\mathrm{CBS+CV}}}{dx} = \frac{dE^{CBS}(\mathrm{HF})}{dx} + \frac{d\Delta E^{CBS}(\mathrm{CCSD(T)})}{dx} + \frac{d\Delta E_{CV}}{dx} \, . \tag{1}$$

The first term on the right-end side of Eq. 1 is the energy gradient of the Hartree-Fock Self-consistent Field (HF-SCF) method extrapolated to the complete basis set (CBS) limit using the exponential formula by Feller [31]. This extrapolation requires the evaluation of the gradient with three different basis sets, which are, in this case, the cc-pVnZ sets with n=T,Q,5 [32]. The second term, i.e. $d\Delta E^{CBS}(\mathrm{CCSD(T)})/dx$, denotes the contribution of the extrapolated CCSD(T) correlation energy gradient. The latter is obtained with the two-point extrapolation formula from ref. [33] and the basis sets employed are cc-pVTZ and cc-pVQZ. Since these two previous terms are computed within the frozen-core (fc-) approximation, the contribution of core-valence is added via the $d\Delta E_{CV}/dx$ term. This is the gradient difference between all-electron (ae-) and fc-computations with the same basis set, i.e. the cc-pCVTZ set [34, 35]. This procedure is implemented in a black-box manner in the `CFOUR` quantum-chemical program [36, 37]. For comparison purposes, the accurate "CBS+CV"equilibrium rotational constants are compared with those obtained with a rather cheap methodology based on extrapolated geometrical parameters (instead of extrapolated gradients). This methodology, first proposed in refs. [38, 39], is here employed in its variant denoted "june-cheap" scheme (hereafter junChS), which has recently been proposed for energetic evaluations (see ref. [40] for further details). In this approach, while the starting point is still a fc-CCSD(T) computation, the CBS and CV corrections are incorporated using the cheaper Møller-Plesset perturbation theory to the second order (MP2) [41].

The vibrational corrections to the equilibrium rotational constants have been obtained within a generalized vibrational perturbation theory (GVPT2) treatment [42]. The required cubic force field has been evaluated using MP2 in conjunction with the cc-pVTZ basis set. The cubic force-field calculations have been carried out on top of the corresponding optimized geometries with the Gaussian16 rev. C01 suite of programs [43]. As already mentioned, the simulation of rotational spectra also requires the knowledge of the centrifugal distortion constants. The most important contribution is due to the quartic terms, but an improved prediction of the spectrum is obtained by also including higher-order distortion constants such as the sextic terms. The quartics have been derived from an analytically evaluated harmonic force field at the ae-CCSD(T)/cc-pCVTZ level of theory. Instead, the sextic centrifugal distortions constants have been obtained as a byproduct of the anharmonic force field calculations carried out for the vibrational corrections to the rotational constants.

The computations described above give also access to the accurate prediction of the infrared spectrum of CPCA. Indeed, the fundamental bands can be derived by augmenting the harmonic vibrational frequencies at the ae-CCSD(T)/cc-pCVTZ level, $\omega^{har}_{i,CC}$, with the anharmonic contributions at the fc-MP2/cc-pVTZ level, $\Delta\nu_{MP2}$, ac-

cording to the expression:

$$\nu_{i,best} = \omega^{har}_{i,CC} + \Delta\nu_{i,MP2} = \omega^{har}_{i,CC} + (\nu^{anh}_{i.MP2} - \omega^{har}_{i,MP2}) \; . \tag{2}$$

In the equation above, i denotes the i-th normal mode, and *har* and *anh* stand for harmonic and anharmonic, respectively.

To investigate the relative stability of the two conformers, the starting point is the "CBS+CV" energy obtained for each conformer from the corresponding optimization procedure (see Eq. 1). While the extrapolation to the CBS limit reduces the one-electron error due to the truncation of the basis set, further energy corrections have been incorporated in order to account for higher-order excitations and thus reduce the N-electron error. Actually, we considered: (i) the full contribution of triple excitations, which has been computed as the difference between CCSDT and CCSD(T) calculations with a cc-pVTZ basis set ($\Delta E_{\rm fT}$) [44, 45], CCSDT standing for CC singles, doubles and triples; (ii) the contribution due to the quadruple excitations ($\Delta E_{\rm (Q)}$), which has been included via the CCSDT(Q) method, i.e. CC singles, doubles, triples and a perturbative treatment of quadruples [46–48]. This corrective term has been evaluated as energy difference between CCSDT and CCSDT(Q), both with the cc-pVDZ basis. Finally, the energetic scheme also includes: (iii) the diagonal Born-Oppenheimer correction obtained at the HF/aug-cc-pVTZ level ($\Delta E_{\rm DBOC}$) [49, 50]; (iv) scalar relativistic effects computed using perturbation theory at the CCSD(T)/aug-cc-pCVTZ level ($\Delta E_{\rm rel}$) [51, 52]; (v) the anharmonic ZPE correction (ΔE_{ZPE}). This latter has been obtained in a hybrid fashion, thereby summing the ae-CCSD(T)/cc-pCVTZ harmonic ZPE to the anharmonic ZPE contribution at the fc-MP2/cc-pVTZ level. By summarizing, the best energy for both conformers (E_{best}) has been evaluated as:

$$\begin{aligned} E_{best} = & E^{CBS}(\text{HF}) + \Delta E^{^{CBS}}(\text{CCSD(T)}) + \Delta E_{\rm CV} + \Delta E_{\rm fT} \\ & + \Delta E_{\rm (Q)} + \Delta E_{\rm DBOC} + \Delta E_{\rm rel} + \Delta E_{ZPE} \; . \end{aligned} \tag{3}$$

The composite scheme described above is denoted as HEAT-like [53–55] because it is based on, and actually very similar to, the HEAT protocol [56–58], which is able to provide formation enthalpies with a sub-kJ/mol accuracy.

A final note on the rotational interconversion barrier of the *syn*-*anti* conformers is deserved. The transition state of the interconversion has been located on the fc-MP2/cc-pVTZ PES, but we were unable to further improve the structure at the CCSD(T) or even higher level. Therefore, the interconversion barrier has only been estimated at the fc-MP2/cc-pVTZ level, and ZPE corrected using the corresponding harmonic contribution.

4. Results and Discussion

4.1. Rotational Analysis

A total of 946 newly observed rotational transitions have been assigned for both CPCA conformers. They comprise 363 a-type and 40 c-type lines of *anti*-CPCA and 236 a-type and 307 b-type transitions of *syn*-CPCA. Two data-sets, incorporating the newly measured frequencies and the literature data [15, 16], have been analysed in a weighted least-squares procedure employing the standard semi-rigid Watson Hamiltonian in its symmetric reduction [59] and using distortion terms up to the $10^{\rm th}$ power in the

angular momentum operators. The fitting procedure has been performed with the `SPFIT` subroutine of the `CALPGM` suite [60] and with `PGOPHER` [24]. The complete list of rotational transition employed is reported in the Supporting Material (SM).

As evident from Table 1, the rotational constants of both CPCA forms have been obtained with great precision and agree very well with our *ab initio* computations, the discrepancy being well below 0.1 %. Moreover, the accuracy of experimental results has been improved by one to two orders of magnitudes with the respect to previous determinations [15, 16]. A good agreement is also observed between "CBS+CV" equilibrium rotational constants and those obtained with the junChS scheme. Indeed, the junChS approach once augmented by vibrational corrections gives $A = 11427.37$, $B = 4000.43$ and $C = 3855.75$ MHz for the *syn* and $A = 15899.55$, $B = 3198.28$, and $C = 3044.04$ MHz for the *anti*. These can be compared with the "CBS+CV" counterpart reported in Table 1, the relative error being always well within 0.5%. Furthermore, the junChS values are within 0.1-0.2% error with respect to the experimental ones, thus proving that also the junChS scheme is able to provide accurate equilibrium structural parameters. The CBS+CV geometries are reported in the SM.

As far as the quartic centrifugal distortion constants are concerned, the agreement between experimental and theoretical values is around 1–10 %, as expected at this level of theory [8, 61, 62]. On the experimental side, thanks to the observation of high J and K_a transitions, the accuracy achieved for these parameters supersedes the quality of literature data [15]. The whole set of sextic centrifugal distortion parameters has been experimentally determined for *syn*-CPCA, while only two diagonal constants (H_{JK} and H_{KJ}) could be optimized for *anti*-CPCA, with the remaining sextic parameters kept fixed at our computed values. A few additional higher-order constants were needed in order to fit all the observed transitions at their experimental accuracy. The complete set of spectroscopic constants is listed in Table 1 together with their computed counterpart and the fit statistics.

4.2. Vibrational Analysis

The re-analysis of the vibrational bands of *syn*- and *anti*-CPCA was carried out with the final purpose of defining the experimental ZPE of the conformers to be used in assessing the relative stability between the two species. The frequencies reported in ref. [13] are our experimental reference and they are compared with our best estimates in Table 2.

For the *syn* conformer, the fundamental frequencies obtained at the harmonic level are in good agreement with the experimental assignment, with a mean difference of 1.9% and a standard deviation of 3.8%. In this statistics, an outlier is the ν_{26} band, which is predicted by our best harmonic computation at 303.9 cm^{-1} and is instead assigned to a frequency of 340 cm^{-1}. Once the anharmonic contribution is taken into account, the computed vibrational frequency becomes $\sim$300 cm^{-1}, thus being further displaced from the experimental value. The ν_{26} band corresponds to the out-of-plane bending mode of the HCO group occurring together with a ring motion; thus, it could be considered a large amplitude motion, which is not well described by the perturbative approach employed in our anharmonic computations. However, such an explanation does not justify the anomalously large discrepancy already present at the harmonic level. Therefore, our conclusion is that the experimental value was misassigned. It should be noted that this part of the vibrational spectrum is rather congested because of the presence of the ν_{26} fundamental of the *anti* species, which was also assigned at

Table 1. Ground-state rotational and centrifugal distortion constants of CPCA conformers.

		syn[a]		*anti*[b]	
Constant	Unit	Exp.[c]	Theo.[d]	Exp.[c]	Theo.[d]
A	MHz	11417.3216(2)	11425.46	15885.571(2)	15895.71
B	MHz	3994.1865(8)	3995.23	3195.10231(6)	3196.58
C	MHz	3849.9305(1)	3850.98	3040.94005(6)	3042.54
D_J	kHz	3.7347(2)	3.506	0.509224(9)	0.503
D_{JK}	kHz	1.2497(2)	1.320	12.5708(4)	12.2
D_K	kHz	-3.3082(2)	-3.117	0.82(2)	0.859
d_1	kHz	-1.3390(2)	-1.201	-0.01927(1)	-0.0161
d_2	kHz	-0.7694(1)	-0.777	-0.005715(8)	-0.0049
H_J	mHz	4.8(2)	5.521	0.031	0.031
H_{JK}	mHz	-13.34(3)	-12.324	73.7(1)	72.
H_{KJ}	mHz	23.1(2)	16.974	-798(1)	-750
H_K	mHz	-14.64(9)	-10.402	690	690
h_1	mHz	8.2(3)	7.207	-0.0007	-0.0007
h_2	mHz	5.2(2)	4.100	0.0660	0.0660
h_3	mHz	-0.74(5)	-0.505	0.0035	0.0035
L_{JK}	mHz			0.0076(4)	
L_{KKJ}	mHz			-0.0830(9)	
M_{KJ}	μHz			0.0034(2)	
M_{KKJ}	μHz			-0.0103(3)	
No. of lines		1249		569	
$J_{\max}, K_{\mathrm{a}\max}$		76, 31		48, 43	
rms	kHz	34.3		22.2	
σ		0.99		0.92	

[a] Parameters are given in the III^r representation. [b] Parameters are given in the I^r representation. [c] Values in parenthesis denote 1σ uncertainties in unit of the last quoted digit. Values given without error have been kept fixed at the corresponding computed values [d] "CBS+CV" equilibrium rotational constants corrected for the vibrational contribution at the fc-MP2/cc-pVTZ level.

340 cm^{-1} in ref. [13]. The latter value is in agreement with our best theoretical estimate of 333 cm^{-1}. Since there is room to claim that the ν_{26} modes should be described by the theory with the same accuracy, the experimental frequency of the *syn* conformer should be reconsidered and it probably lies between 290 and 300 cm^{-1}, where some unassigned features were observed in the solid state spectrum [17]. Furthermore, the computational values of these vibrational bands are in agreement with those previously computed in the literature and reported in refs. [15, 20]. For all the other fundamentals of the *syn* conformer, it is evident that the small anharmonic contribution reduces the discrepancy with respect to the experiment by one order of magnitude. If we exclude the ν_{26} band from the statistical consideration, the overall standard deviation reduces to 1.6%, with an averaged mean error of 0.95%.

Table 2. Fundamental frequencies (cm^{-1}) of the *syn* and *anti* conformers of CPCA.

syn								*anti*							
Symmetry	Mode	Harmonic[a]	Anharm. Corr.[b]	Best	Experiment[c]	$\delta\%_{harm}$	$\delta\%_{best}$	Symmetry	Mode	Harmonic[a]	Anharm. Corr.[b]	Best	Experiment[c]	$\delta\%_{harm}$	$\delta\%_{best}$
A′	ν_1	3261.92	-143.10	3118.82	3102	5.16	0.54	A′	ν_1	3254.35	-141.81	3112.54	3085	5.49	0.89
	ν_2	3201.14	-133.15	3067.99	3055	4.78	0.43		ν_2	3210.19	-134.88	3075.30	3063	4.81	0.40
	ν_3	3159.53	-122.20	3037.33	3026	4.41	0.37		ν_3	3156.35	-120.88	3035.48	3010	4.86	0.85
	ν_4	2942.68	-120.80	2821.88	2822	4.28	0.00		ν_4	2882.11	-218.18	2663.93	2840 - 2686[d]	1.48 - 7.3	6.20 - 0.86
	ν_5	1770.90	-32.13	1738.77	1740	1.78	0.07		ν_5	1791.09	-35.10	1755.99	(1722)	4.01	1.97
	ν_6	1504.38	-47.79	1456.59	1443	4.25	0.94		ν_6	1515.50	-50.41	1465.09	(1462)	3.66	0.21
	ν_7	1429.26	-33.49	1395.77	1396	2.38	0.02		ν_7	1439.60	-34.91	1404.59	1398	2.98	0.48
	ν_8	1399.77	-35.79	1363.99	1363	2.70	0.07		ν_8	1353.21	-36.44	1316.76	(1317)	2.75	0.02
	ν_9	1221.40	-28.91	1192.50	1195	2.21	0.21		ν_9	1224.07	-29.50	1194.57	1175	4.18	1.67
	ν_{10}	1106.40	-21.19	1085.21	1074	3.02	1.04		ν_{10}	1189.26	-30.16	1159.10	1197	0.65	3.17
	ν_{11}	1069.79	-20.78	1049.01	1034	3.46	1.45		ν_{11}	1066.93	-28.04	1038.89	1040	2.59	0.11
	ν_{12}	992.41	-30.53	961.88	960	3.38	0.20		ν_{12}	958.67	-33.18	925.49	(926)	3.53	0.06
	ν_{13}	819.48	-12.09	807.39	808	1.42	0.08		ν_{13}	888.69	-14.55	874.14	880	0.99	0.67
	ν_{14}	795.83	-14.61	781.23	783	1.64	0.23		ν_{14}	779.47	-9.23	770.24	784	0.58	1.75
	ν_{15}	676.16	-7.05	669.11	670	0.92	0.13		ν_{15}	502.59	-3.29	499.30	(504)	0.28	0.93
	ν_{16}	247.08	12.03	259.11	256	3.48	1.21		ν_{16}	283.96	3.65	287.61	(291)	2.42	1.17
A″	ν_{17}	3248.67	-143.15	3105.51	3108	4.53	0.08	A″	ν_{17}	3241.17	-142.61	3098.57	3095	4.72	0.12
	ν_{18}	3155.76	-121.59	3034.17	3008	4.91	0.87		ν_{18}	3151.51	-116.78	3034.73	3030	4.01	0.16
	ν_{19}	1465.15	-40.00	1425.15	1426	2.75	0.06		ν_{19}	1477.25	-39.08	1438.17	1434	3.02	0.29
	ν_{20}	1217.51	-28.63	1188.88	1175	3.62	1.18		ν_{20}	1208.67	-27.88	1180.79	1197	0.98	1.35
	ν_{21}	1131.04	-26.46	1104.58	1151	1.73	4.03		ν_{21}	1134.12	-31.72	1102.40	1100	3.10	0.22
	ν_{22}	1101.55	-26.71	1074.84	1082	1.81	0.66		ν_{22}	1090.86	-27.31	1063.55	1080	1.01	1.52
	ν_{23}	1046.86	-24.12	1022.74	1018	2.83	0.47		ν_{23}	1040.77	-23.32	1017.45	1018	2.24	0.05
	ν_{24}	847.95	-9.16	838.78	875	3.09	4.14		ν_{24}	858.61	-36.27	822.35	857	0.19	4.04
	ν_{25}	836.54	-26.00	810.54	820	2.02	1.15		ν_{25}	845.39	-2.32	843.07	804	5.15	4.86
	ν_{26}	303.92	-3.40	300.51	340 - ∼300[d]	10.61 - 0.00	11.61 - 0.00		ν_{26}	336.69	-3.64	333.06	(340)	0.97	2.04
	ν_{27}	116.31	-3.15	113.16	113	2.93	0.14		ν_{27}	130.79	-4.58	126.21	(126)	3.80	0.16

[a] Harmonic values obtained at the ae-CCSD(T)/cc-pCVTZ level of theory.
[b] Anharmonic corrections from fc-MP2/cc-pVTZ computations.
[c] Experimental values from ref. [13]. For the *anti* species, only the values within parentheses are from gas-phase experiments. [d] New assignment from this work.

The vibrational spectrum of the *anti* conformer was measured in the solid phase and only some bands, namely ν_5, ν_6, ν_8, ν_{12}, ν_{15}, ν_{16}, ν_{26}, and ν_{27}, were observed in the gas phase. As noted for the *syn* conformer, the agreement with theoretical harmonic values is good, with a standard deviation of 3.5% and a maximum deviation of 5.5% for ν_1. The anharmonic contribution further reduces the disagreement between computed and experimental transitions, but a non-negligible deterioration is seen for the prediction of the ν_4 band. The latter is associated to the C-H stretching mode of the aldehydic carbon and it was assigned at 2840 cm^{-1}. The harmonic value seems in good agreement with this assignment, predicting the fundamental band at 2882 cm^{-1}. However, once the anharmonicity is introduced, the vibrational band is shifted at lower energy by $\sim$220 cm^{-1}. This could be due to the presence of resonances, which however should be accounted for by the GVPT2 approach. For the *syn* conformer, the same mode is instead well predicted. Since a correction of $\sim$220 cm^{-1} for the ν_4 band is about 8% of its harmonic value, it can be thus considered reliable. Hence, our conclusion is that this vibrational mode was misassigned too. In ref. [14], the authors state that the C-H stretching modes for the *syn* and *anti* have been excited in the 2670-2850 cm^{-1} range to induce the *syn*-*anti* isomerism. In particular, in ref. [14] it is confirmed that the ν_4 of the *syn* conformer lies at 2822 cm^{-1}, but no conclusions are drawn on the two vibrational bands at 2806 and 2686 cm^{-1} excited for the *anti* conformer. In another literature paper [20], the C-H stretching of the aldehydic carbon was assigned at 2806 cm^{-1} using the computed MP2/cc-pVTZ value as reference. However, in the same paper, in analogy to our calculations, the ωB97XD functional predicts the ν_4 band at $\sim$2620 cm^{-1}. Interestingly, this is close to the second value employed by Dian and coworkers [14] to excite the *anti* conformer.

To have a better picture of the vibrational bands between 2500 and 2900 cm^{-1}, a low-resolution FT-IR spectrum of CPCA similar to that reported in ref. [14], was recorded and is shown in Fig. 3 together with the most intense theoretical bands predicted to lie in the same range. In particular, for the *syn* conformer (red features in Fig. 3), the ν_4 fundamental is the most intense band and its assignment is in line with what previously reported in the literature (see Fig. 3). According to our calculations, three equally intense bands are present in the region considered for the *anti* conformer. These are the ν_4 fundamental (2663.9 cm^{-1}), the $2\nu_7$ overtone (2834.7 cm^{-1}), and the $\nu_8 + \nu_7$ combination band (2753.1 cm^{-1}). In the low resolution spectrum, an intense band is observed at 2680 cm^{-1}, which can be safely assigned to the ν_4 fundamental band, in agreement with our computed value and with the band at 2686 cm^{-1} used in ref. [14] to excite *anti*-CPCA. As a consequence of this reassignment, we conclude that the feature observed in ref. [13] at 2840 cm^{-1} and also used in ref. [14] for exciting CPCA is, most likely, the $2\nu_7$ of the *anti* form. The last consideration concerns the strong peak at around 2730 cm^{-1}, which — according to ref. [14] — is a feature resulting from the sum of two different signals. Based on our computations, these are the ν_8+ν_7 combination band of the *anti* form and the $2\nu_7$ overtone of *syn*-CPCA (see Fig. 3).

With the ν_4 band reassigned, we can now calculate the experimental ZPE, assuming this as one half the sum of all fundamental frequencies. Based on the original assignments, the experimental ZPEs obtained from the frequencies of ref. [13] are 232.3 and 231.9 kJ mol^{-1} for the *syn* and *anti* conformer, respectively. These values becomes 232.1 and 231.0 kJ mol^{-1}, respectively, if one considers the reassignments of ν_4 (*anti*) and ν_{26} (*syn*) inferred in this work, with the ν_4 fundamental strongly affecting the value of the ZPE for the *anti* conformer. The experimental ZPEs are in roughly good agreement with those obtained from the best computational estimate, namely

236.7 (*syn*) and 236.3 kJ mol^{-1} (*anti*), which have been obtained by summing the harmonic ZPE at the ae-CCSD(T)/cc-pCVTZ level with the anharmonic-ZPE contribution at the fc-MP2/cc-pVTZ level. As a final note, the ZPE always makes the *anti* conformer more stable than the *syn* form, the ZPE difference being 0.4/1.1 kJ mol^{-1} (theory/experiment) in favour of the *anti* species.

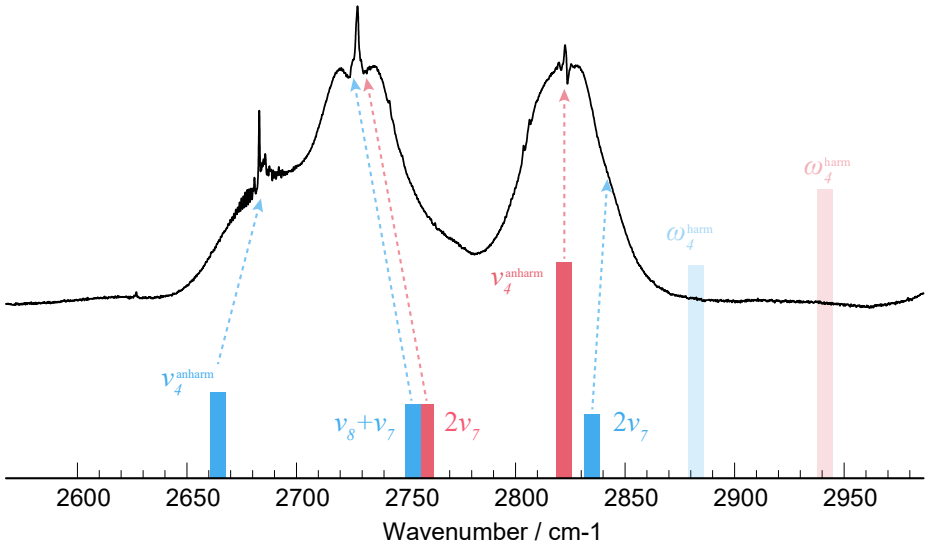

Figure 3. Low-resolution infrared spectrum of CPCA (black plot) in the 2500-2900 cm^{-1} range together with the computed vibrational features of the *syn* form (red bars) and of the *anti* conformer (blue bars).

4.3. Relative stability

As anticipated in Section 1, the relative stability of different conformational isomers can be evaluated experimentally through gas-phase intensity measurements. To exploit the recorded millimetre-wave spectra for such purpose, the partition function and dipole transition moment are required. The former has been derived as described in the following by considering the electronic partition function unitary. Thus, only rotational and vibrational partition functions have to be derived. The dipole transition moment is estimated from the components of the permanent electric dipole moment. The latter were determined via Stark effect measurements by Volltrauer and Schwendeman [16], and their values are: $\mu_a = 2.02(1)$ D and $\mu_b = 1.86(1)$ D for *syn*-CPCA, $\mu_a = 3.22(1)$ D and $\mu_c = 0.49(1)$ D for *anti*-CPCA. The components not reported vanish by symmetry.

The rotational partition function $Q_{\rm rot}(T)$ can be computed to a very good approximation as:

$$Q_{\rm rot}(T) = 5.3311 \times 10^6 \sqrt{\frac{T^3}{(A\,B\,C)}} \qquad (4)$$

with the A, B, and C constants being expressed in MHz and the temperature T given in K. The numerical factor accounts for all fundamental constants and conversion factors required. Using our newly determined rotational constants, Eq. (4) leads to

66111 for *syn*-CPCA and 70510 for *anti*-CPCA at 300 K. Alternatively, $Q_{\rm rot}$ can be computed analytically by summing up the contributions of each rotational level within a given energy threshold. We performed this calculation using the `SPCAT` code [60], and limiting the J and K_a values to 160 and 70, respectively. Within these boundaries, the calculation is fully converged and gives $Q_{\rm rot}^{(syn)} = 66291$ and $Q_{\rm rot}^{(anti)} = 70646$, these values being in perfect agreement with those derived from Eq. (4).

An analytical evaluation of the vibrational partition function $Q_{\rm vib}(T)$ is in most cases impossible, thus requiring the use of approximate solutions. Based on refs. [63, 64], the following harmonic formulation is employed:

$$Q_{\rm vib}(T) = \prod_{i=1}^{3N-6} \left(1 - e^{-\frac{h\nu_i}{k_B T}}\right)^{-1} , \qquad (5)$$

where the sum runs over the normal coordinates, with ν_i being the anharmonic vibrational frequency of the i-th normal mode. Using Eq. (5) in combination with either our best computed anharmonic frequencies or the experimental ones, we get average values of $Q_{\rm vib}^{(syn)} = 5.2$ and $Q_{\rm vib}^{(anti)} = 4.5$ at 300 K.

The combination of the partition function and dipole transition moment has been used to derive the intensity of few tens of transitions for each conformer, thus allowing to retrieve the population ratio from peak integration. For this evaluation, the transitions chosen lie very close in the spectrum and, thus, were recorded in similar conditions. Unfortunately, the results obtained in this manner are rather inconclusive, since the mean population ratio, *syn*/*anti*, is 1 ± 0.2. Cabezas et al. [15] estimated, in a similar fashion as in our work, their experimental population ratio, then suggesting that the *anti* conformer is the lowest in energy by 0.53 kJ mol^{-1}. However, their vibrational partition function for the *syn* form was derived considering that the ν_{27} band lies at 123 cm^{-1}, while experimentally it is observed at 113 cm^{-1}. This frequency is also well predicted by our best computational estimate at 113.16 cm^{-1}. Therefore, the stability of 0.53 kJ mol^{-1} for the *anti* conformer needs to be revised and also their statistics might lead to a rather inconclusive value.

While experimental considerations do not lead to a clear conclusion on the stability order of the two conformers, the theoretical line seems to be better defined. The *syn* species is predicted to be more stable than the *anti* by 1.58 kJ mol^{-1} at the fc-MP2/cc-pVTZ level. A similar value is also obtained at the ae-CCSD(T)/cc-pCVTZ level of theory (1.13 kJ mol^{-1}), but the "CBS+CV" approach reduces the energy difference to 0.49 kJ mol^{-1}. The contribution of full treatment of triple excitations ($\Delta E_{\rm fT}$) favours the *anti* conformer by 0.09 kJ mol^{-1}, while the $\Delta E_{\rm (Q)}$, $\Delta E_{\rm DBOC}$ and $\Delta E_{\rm rel}$ corrections still favour the *anti* form but by only 0.01 kJ mol^{-1}. Overall, at the equilibrium, the *syn* conformer lies lower in energy than the *anti* species by only 0.38 kJ mol^{-1}. As inferred in the previous section, the ZPE favours the stability of the *anti* conformer. Using our best estimate of the ZPEs (see above) would lead to the *anti* conformer being 0.002 kJ mol^{-1} more stable than the *syn* form. If the experimentally derived ZPEs are employed (232.1 and 231.0 kJ mol^{-1}), the stability of *anti*-CPCA becomes more evident, this being 0.71 kJ mol^{-1} below the *syn* conformer. All the derivations discussed in this section are collected and compared in Table 3, where other determinations from the literature are also reported.

A last note is on the interconversion barrier between *anti* and *syn* computed at the fc-MP2/cc-pVTZ level. Using equilibrium values, this is 24.6 kJ mol^{-1} for the *anti* $\rightarrow TS \rightarrow$ *syn* process and 25.6 kJ mol^{-1} for the reversed one. These values are

in agreement with previous estimates [16, 18]. However, the error associated to the fc-MP2/cc-pVTZ level of theory is greater than the difference of 1 kJ mol^{-1} between the two interconversion barriers. The structure of the TS involved in the interconversion is reported in the SM.

Table 3. Relative energies (kJ mol^{-1}) between *syn* and *anti* conformers.

Energy	$\Delta E(syn - anti)$
Best comp.[a]	-0.38
Best comp.+ZPE$^{b}_{\text{anh}}$	0.002
Best comp.+ZPE$^{c}_{\text{exp}}$	0.71
Theo.[d]	0.02
Exp. (This work)	0 ± 0.46
Exp. MW[e]	0.12 ± 0.24
Exp. IR[f]	-0.72
Exp. mm[g]	0.53

[a]Best equilibrium value obtained in this work. [b]ZPE correction derived from the harmonic ZPE at the ae-CCSD(T)/cc-pCVTZ level of theory corrected for the fc-MP2/cc-pVTZ anharmonic contribution. [c]Experimental ZPE obtained as one half the sum of the vibrational experimental frequencies, considering the reassignments suggested is this work. [d]Best theoretical value of ref. [20]. [e]Experimental value from ref. [16]. [f]Experimental value from ref. [13] [g]Experimental value from ref. [15].

5. Conclusion

The conformational stability of cyclopropanecarboxaldehyde was re-investigated from the computational and experimental point of view. The computational strategies employed for the characterization are based on the determination of accurate "CBS+CV" structural parameters on top of which the electronic energies were further refined to account for others contributions, such as relativistic effects and quadruple excitations. The computational results at the equilibrium predict the *syn* conformer to be the most stable by about 0.4 kJ mol^{-1}. Yet, the inclusion of the vibrational zero-point energies leads to a reversed stability, with the *anti* form located 0.002 kJ mol^{-1} below the *syn* conformer.

The computational investigation also provided the determination of several spectroscopic parameters, which have been used to interpret the new experimental measurements, reported in this work, in the field of rotational spectroscopy. In particular, for the *anti*-CPCA some 400 new rotational transitions have been assigned, while for the *syn*-CPCA the newly assigned rotational frequencies are about 500. The global analysis of these new lines together with those previously reported in the literature [15, 16] led to a fit with a standard deviation of 0.99 for *syn* and 0.92 for *anti*.

The vibrational spectrum of both conformers of CPCA reported in ref. [13] was re-analysed in view of the accurate vibrational frequencies computed in this work and two reassignment were proposed. In particular, for the *syn* conformer the ν_{26} fundamental was found to lie at $\sim$300 cm^{-1}, instead of 340 cm^{-1} as reported in ref. [13]. For the *anti* form, a re-assignment of the ν_4 fundamental band at 2686 cm^{-1} was suggested based both on our computations and Dian et al. [14] data.

The new mm-wave measurement were also used to experimentally derive the relative stability of the two conformers via the mean population ratio obtained from the

integrated intensity of several lines. This was accomplished by comparing the experimental intensity with the predicted one, which was obtained using the rotational and vibrational partition functions. While the former is straightforwardly derived from experimental data, i.e. the rotational spectroscopic parameters, of this work, the vibrational partition function has been estimated using both the original experimental fundamental bands [17] and those reassigned. Unfortunately, the experimental results on the relative stability are quite inconclusive, since the mean population ratio *syn*/*anti*was found to be 1 ± 0.2, which in energy terms is translated to 0 ± 0.46 kJ mol^{-1}. This result is strongly affected by the vibrational partition function and by the assumption made for its derivation. Furthermore, the $Q_{\mathrm{vib}}^{syn}(T)$ is greatly influenced by the lowest vibrational fundamental, which lies at 113 cm^{-1} based on experiment and on our computations, which was however predicted at 123 cm^{-1} in another work, thus affecting the relative stability determination. Therefore, our conclusion is that a definitive answer on the stability of the two CPCA conformers in the gas phase can be only obtained when further improvements of the experimental vibrational features will be reported, with our work currently reporting the best rotational analysis of both conformers and the best accurate computed values for the vibrational spectra and equilibrium quantities.

6. Acknowledgement

This study was supported by Bologna University (RFO funds). The SMART@SNS Laboratory (http://smart.sns.it) is acknowledged for providing high-performance computing facilities. Support by the Italian Space Agency (ASI; 'Life in Space' project, N. 2019-3-U.0) is also acknowledged.

References

[1] G. P. Moss, "Basic terminology of stereochemistry (IUPAC Recommendations 1996)," *Pure Appl. Chem.*, vol. 68, pp. 2193–2222, 1996.

[2] M. Born and R. Oppenheimer, "Zur quantentheorie der molekeln," *Ann. Phys. (Berl.)*, vol. 389, pp. 457–484, 1927.

[3] L. S. Bartell and J. P. Guillory, "Electron-diffraction study of the structure and internal rotation of cyclopropyl carboxaldehyde," *J. Chem. Phys.*, vol. 43, pp. 647–653, 1965.

[4] R. L. Hudson and F. M. Coleman, "Solid-state isomerization and infrared band strengths of two conformational isomers of cyclopropanecarboxaldehyde, a candidate interstellar molecule," *ACS Earth and Space Chem.*, vol. 3, pp. 1182–1188, 2019.

[5] J. M. Hollas, *Modern spectroscopy*. John Wiley & Sons, 2004.

[6] V. Barone, S. Alessandrini, M. Biczysko, J. R. Cheeseman, D. C. Clary, A. B. McCoy, R. J. DiRisio, F. Neese, M. Melosso, and C. Puzzarini, "Computational molecular spectroscopy," *Nat. Rev. Methods Primers*, vol. 1, no. 38, 2021.

[7] V. Barone, M. Biczysko, J. Bloino, and C. Puzzarini, "Glycine conformers: a never-ending story?," *Phys. Chem. Chem. Phys.*, vol. 15, pp. 1358–1363, 2013.

[8] C. Puzzarini, J. Bloino, N. Tasinato, and V. Barone, "Accuracy and interpretability: The devil and the holy grail. new routes across old boundaries in computational spectroscopy," *Chem. Rev.*, vol. 119, pp. 8131–8191, 2019.

[9] E. R. Alonso, M. Fusè, I. León, C. Puzzarini, J. L. Alonso, and V. Barone, "Exploring the maze of cycloserine conformers in the gas phase guided by microwave spectroscopy and quantum chemistry," *J. Phys. Chem. A*, vol. 125, pp. 2121–2129, 2021.

[10] I. Peña, M. E. Sanz, J. C. López, and J. L. Alonso, "Preferred conformers of proteinogenic glutamic acid," *J. Am. Chem. Soc.*, vol. 134, pp. 2305–2312, 2012.
[11] A. Simão, C. Cabezas, I. León, E. R. Alonso, S. Mata, and J. L. Alonso, "Elucidating the multiple structures of pipecolic acid by rotational spectroscopy," *Phys. Chem. Chem. Phys.*, vol. 21, pp. 4155–4161, 2019.
[12] W. Li, L. Spada, N. Tasinato, S. Rampino, L. Evangelisti, A. Gualandi, P. G. Cozzi, S. Melandri, V. Barone, and C. Puzzarini, "Theory meets experiment for noncovalent complexes: The puzzling case of pnicogen interactions," *Angew. Chem. Int. Ed.*, vol. 57, pp. 13853–13857, 2018.
[13] J. Durig, F. Feng, T. Little, and A.-Y. Wang, "Conformational stability, barriers to internal rotation, structural parameters, ab initio calculations, and vibrational assignment of cyclopropanecarboxaldehyde," *Struct. Chem.*, vol. 3, pp. 417–428, 1992.
[14] B. C. Dian, G. G. Brown, K. O. Douglass, and B. H. Pate, "Measuring picosecond isomerization kinetics via broadband microwave spectroscopy," *Science*, vol. 320, pp. 924–928, 2008.
[15] Cabezas, C., Neeman, E. M., Tercero, B., Bermúdez, C., and Cernicharo, J., "Comprehensive rotational study and astronomical search for cyclopropanecarboxaldehyde," *A&A*, vol. 645, p. A75, 2021.
[16] H. Volltrauer and R. Schwendeman, "Microwave spectra, dipole moments, and torsional potential constants of cis-and trans-cyclopropanecarboxaldehyde," *J. Chem. Phys.*, vol. 54, pp. 260–267, 1971.
[17] J. Durig and T. Little, "Vibrational and conformational studies of cyclopropanecarboxaldehyde," *Croat. Chem. Acta*, vol. 61, pp. 529–549, 1988.
[18] D. M. Pawar and E. A. Noe, "Dynamic nmr study of cyclopropanecarbaldehyde. comparison of the conjugating abilities of the cyclopropyl and phenyl groups," *J. Org. Chem.*, vol. 63, pp. 2850–2853, 1998.
[19] M. Schnell, "Broadband rotational spectroscopy for molecular structure and dynamics studies," *Z. Phys. Chem.*, vol. 227, pp. 1–22, 2013.
[20] C. Trindle, E. A. Bleda, and Z. Altun, "Structure and energetics of cyclopropane carboxaldehyde," *Int. J. Quant. Chem.*, vol. 113, pp. 1155–1161, 2013.
[21] X.-J. Hou and M.-B. Huang, "Internal rotations of vinylcyclopropane, cyclopropanecarboxaldehyde, and cyclopropanecarboxylic acid: a DFT B3LYP study," *J. Mol. Struct.: THEOCHEM*, vol. 585, pp. 93–104, 2002.
[22] M. Melosso, B. Conversazioni, C. Degli Esposti, L. Dore, E. Cané, F. Tamassia, and L. Bizzocchi, "The pure rotational spectrum of $^{15}ND_2$ observed by millimetre and submillimetre-wave spectroscopy," *J. Quant. Spectrosc. Ra.*, vol. 222, pp. 186–189, 2019.
[23] M. Melosso, L. Bizzocchi, F. Tamassia, C. Degli Esposti, E. Canè, and L. Dore, "The rotational spectrum of ^{15}ND. Isotopic-independent Dunham-type analysis of the imidogen radical," *Phys. Chem. Chem. Phys.*, vol. 21, pp. 3564–3573, 2019.
[24] C. M. Western, "Pgopher: A program for simulating rotational, vibrational and electronic spectra," *J. Quant. Spectrosc. Ra.*, vol. 186, pp. 221–242, 2017.
[25] C. Puzzarini, J. F. Stanton, and J. Gauss, "Quantum-chemical calculation of spectroscopic parameters for rotational spectroscopy," *Int. Rev. Phys. Chem.*, vol. 29, pp. 273–367, 2010.
[26] C. Puzzarini, "Rotational spectroscopy meets theory," *Phys. Chem. Chem. Phys.*, vol. 15, pp. 6595–6607, 2013.
[27] C. Puzzarini, M. Heckert, and J. Gauss, "The accuracy of rotational constants predicted by high-level quantum-chemical calculations. I. molecules containing first-row atoms," *J. Chem. Phys.*, vol. 128, p. 194108, 2008.
[28] I. Shavitt and R. J. Bartlett, "Many-body methods in chemistry and physics," *Many-Body Methods in Chemistry and Physics, 1st ed. Cambrige, Cambridge University Press*, 2009.
[29] K. Raghavachari, G. W. Trucks, J. A. Pople, and M. Head-Gordon, "A fifth-order perturbation comparison of electron correlation theories," *Chem. Phys. Lett.*, vol. 157, pp. 479–483, 1989.
[30] M. Heckert, M. Kállay, and J. Gauss, "Molecular equilibrium geometries based on coupled-

cluster calculations including quadruple excitations," *Mol. Phys.*, vol. 103, pp. 2109–2115, 2005.

[31] D. Feller, "The use of systematic sequences of wave functions for estimating the complete basis set, full configuration interaction limit in water," *J. Phys. Chem.*, vol. 98, pp. 7059–7071, 1993.

[32] T. H. Dunning Jr., "Gaussian basis sets for use in correlated molecular calculations. I. The atoms boron through neon and hydrogen," *J. Chem. Phys.*, vol. 90, pp. 1007–1023, 1989.

[33] T. Helgaker, W. Klopper, H. Koch, and J. Noga, "Basis-set convergence of correlated calculations on water," *J. Phys. Chem.*, vol. 106, p. 9639, 1997.

[34] K. A. Peterson and T. H. Dunning Jr., "Accurate correlation consistent basis sets for molecular core-valence correlation effects: The second row atoms Al-Ar, and the first row atoms B-Ne revisited," *J. Chem. Phys.*, vol. 117, pp. 10548–10560, 2002.

[35] D. E. Woon and T. H. Dunning Jr, "Gaussian basis sets for use in correlated molecular calculations. V. Core-valence basis sets for boron through neon," *J. Chem. Phys.*, vol. 103, pp. 4572–4585, 1995.

[36] J. F. Stanton, J. Gauss, L. Cheng, M. E. Harding, D. A. Matthews, and P. G. Szalay, "CFOUR, Coupled-Cluster techniques for Computational Chemistry, a quantum-chemical program package." With contributions from A.A. Auer, R.J. Bartlett, U. Benedikt, C. Berger, D.E. Bernholdt, Y.J. Bomble, O. Christiansen, F. Engel, R. Faber, M. Heckert, O. Heun, M. Hilgenberg, C. Huber, T.-C. Jagau, D. Jonsson, J. Jusélius, T. Kirsch, K. Klein, W.J. Lauderdale, F. Lipparini, T. Metzroth, L.A. Mück, D.P. O'Neill, D.R. Price, E. Prochnow, C. Puzzarini, K. Ruud, F. Schiffmann, W. Schwalbach, C. Simmons, S. Stopkowicz, A. Tajti, J. Vázquez, F. Wang, J.D. Watts and the integral packages MOLECULE (J. Almlöf and P.R. Taylor), PROPS (P.R. Taylor), ABACUS (T. Helgaker, H.J. Aa. Jensen, P. Jørgensen, and J. Olsen), and ECP routines by A. V. Mitin and C. van Wüllen. For the current version, see http://www.cfour.de.

[37] D. A. Matthews, L. Cheng, M. E. Harding, F. Lipparini, S. Stopkowicz, T.-C. Jagau, P. G. Szalay, J. Gauss, and J. F. Stanton, "Coupled-cluster techniques for computational chemistry: The cfour program package," *J. Chem. Phys.*, vol. 152, p. 214108, 2020.

[38] C. Puzzarini, "Extrapolation to the complete basis set limit of structural parameters: Comparison of different approaches," *The Journal of Physical Chemistry A*, vol. 113, no. 52, pp. 14530–14535, 2009.

[39] C. Puzzarini and V. Barone, "Extending the molecular size in accurate quantum-chemical calculations: The equilibrium structure and spectroscopic properties of uracil," *Phys. Chem. Chem. Phys.*, vol. 13, no. 15, pp. 7189–7197, 2011.

[40] S. Alessandrini, V. Barone, and C. Puzzarini, "Extension of the "Cheap" composite approach to noncovalent interactions: The jun-ChS scheme," *J. Chem. Theory Comput.*, vol. 16, pp. 988–1006, 2019.

[41] C. Møller and M. S. Plesset, "Note on an approximation treatment for many-electron systems," *Phys. Rev*, vol. 46, pp. 618–622, 1934.

[42] M. Piccardo, J. Bloino, and V. Barone, "Generalized vibrational perturbation theory for rotovibrational energies of linear, symmetric and asymmetric tops: Theory, approximations, and automated approaches to deal with medium-to-large molecular systems," *Int. J. Quant. Chem.*, vol. 115, pp. 948–982, 2015.

[43] M. J. Frisch, G. W. Trucks, H. B. Schlegel, G. E. Scuseria, M. A. Robb, J. R. Cheeseman, G. Scalmani, V. Barone, G. A. Petersson, H. Nakatsuji, and et al., "Gaussian 16 Revision C.01," 2016. Gaussian Inc. Wallingford CT.

[44] J. Noga and R. J. Bartlett, "The full CCSDT model for molecular electronic structure," *J. Chem. Phys.*, vol. 86, pp. 7041–7050, 1987.

[45] G. E. Scuseria and H. F. Schaefer III, "A new implementation of the full CCSDT model for molecular electronic structure," *Chem. Phys. Lett.*, vol. 152, pp. 382–386, 1988.

[46] M. Kállay and J. Gauss, "Approximate treatment of higher excitations in coupled-cluster theory," *J. Chem. Phys.*, vol. 123, p. 214105, 2005.

[47] M. Kállay and J. Gauss, "Approximate treatment of higher excitations in coupled-cluster theory. II. Extension to general single-determinant reference functions and improved approaches for the canonical Hartree–Fock case," *J. Chem. Phys.*, vol. 129, p. 144101, 2008.
[48] Y. J. Bomble, J. F. Stanton, M. Kállay, and J. Gauss, "Coupled-cluster methods including noniterative corrections for quadruple excitations," *J. Chem. Phys.*, vol. 123, p. 054101, 2005.
[49] N. C. Handy, Y. Yamaguchi, and H. F. Schaefer III, "The diagonal correction to the Born–Oppenheimer approximation: its effect on the singlet–triplet splitting of CH_2 and other molecular effects," *J. Chem. Phys.*, vol. 84, pp. 4481–4484, 1986.
[50] R. A. Kendall, T. H. Dunning Jr, and R. J. Harrison, "Electron affinities of the first-row atoms revisited. Systematic basis sets and wave functions," *J. Chem. Phys.*, vol. 96, pp. 6796–6806, 1992.
[51] R. D. Cowan and D. C. Griffin, "Approximate relativistic corrections to atomic radial wave functions," *J. Opt. Soc. Am.*, vol. 66, pp. 1010–1014, 1976.
[52] W. Klopper, "Simple recipe for implementing computation of first-order relativistic corrections to electron correlation energies in framework of direct perturbation theory," *J. Comp. Chem.*, vol. 18, pp. 20–27, 1997.
[53] C. Puzzarini and V. Barone, "The challenging playground of astrochemistry: an integrated rotational spectroscopy–quantum chemistry strategy," *Phys. Chem. Chem. Phys.*, vol. 22, pp. 6507–6523, 2020.
[54] J. Lupi, C. Puzzarini, C. Cavallotti, and V. Barone, "State-of-the-art quantum chemistry meets variable reaction coordinate transition state theory to solve the puzzling case of the H2S + Cl system," *J. Chem. Theory Comput.*, vol. 16, no. 8, pp. 5090–5104, 2020.
[55] C. Puzzarini, Z. Salta, N. Tasinato, J. Lupi, C. Cavallotti, and V. Barone, "A twist on the reaction of the CN radical with methylamine in the interstellar medium: new hints from a state-of-the-art quantum-chemical study," *MNRAS*, vol. 496, pp. 4298–4310, 2020.
[56] A. Tajti, P. G. Szalay, A. G. Császár, M. Kállay, J. Gauss, E. F. Valeev, B. A. Flowers, J. Vázquez, and J. F. Stanton, "Heat: High accuracy extrapolated ab initio thermochemistry," *J. Chem. Phys.*, vol. 121, no. 23, pp. 11599–11613, 2004.
[57] Y. J. Bomble, J. Vázquez, M. Kállay, C. Michauk, P. G. Szalay, A. G. Császár, J. Gauss, and J. F. Stanton, "High-accuracy extrapolated ab initio thermochemistry. ii. minor improvements to the protocol and a vital simplification," *The Journal of Chemical Physics*, vol. 125, no. 6, p. 064108, 2006.
[58] M. E. Harding, J. Vázquez, B. Ruscic, A. K. Wilson, J. Gauss, and J. F. Stanton, "High-accuracy extrapolated ab initio thermochemistry. III. Additional improvements and overview," *The Journal of Chemical Physics*, vol. 128, p. 114111, 2008.
[59] J. K. G. Watson, "Aspects of Quartic and Sextic Centrifugal Effects on Rotational Energy Levels," in *Vibrational Spectra and Structure* (J. R. Durig, ed.), pp. 1–89, New York, NY: Elsevier, 1977.
[60] H. M. Pickett, "The fitting and prediction of vibration-rotation spectra with spin interactions," *J. Mol. Spectrosc.*, vol. 148, pp. 371–377, 1991.
[61] C. Puzzarini, G. Cazzoli, and J. Gauss, "The rotational spectra of hd17o and d217o: Experiment and quantum-chemical calculations," *The Journal of Chemical Physics*, vol. 137, no. 15, p. 154311, 2012.
[62] S. Alessandrini, J. Gauss, and C. Puzzarini, "Accuracy of rotational parameters predicted by high-level quantum-chemical calculations: case study of sulfur-containing molecules of astrochemical interest," *J. Chem. Theory and Comput.*, vol. 14, pp. 5360–5371, 2018.
[63] A. D. Isaacson, D. G. Truhlar, K. Scanlon, and J. Overend, "Tests of approximation schemes for vibrational energy levels and partition functions for triatomics: H_2O and SO_2," *J. Chem. Phys.*, vol. 75, no. 6, pp. 3017–3024, 1981.
[64] D. G. Truhlar and A. D. Isaacson, "Simple perturbation theory estimates of equilibrium constants from force fields," *J. Chem. Phys.*, vol. 94, no. 1, pp. 357–359, 1991.